SUPPLEMENTARY MATERIAL

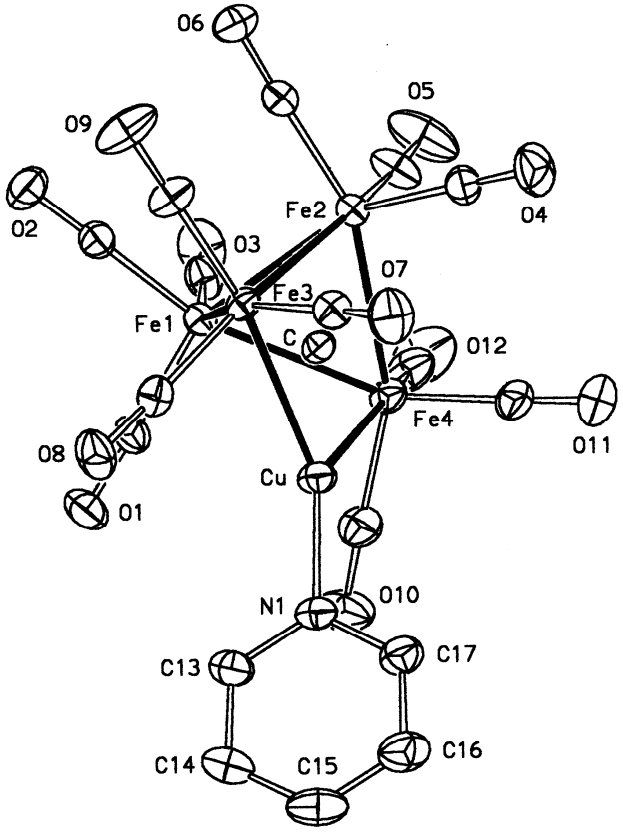

Figure S1 – The solid state structure of $[Fe_4C(CO)_{12}Cupy]^-$**, (5).**

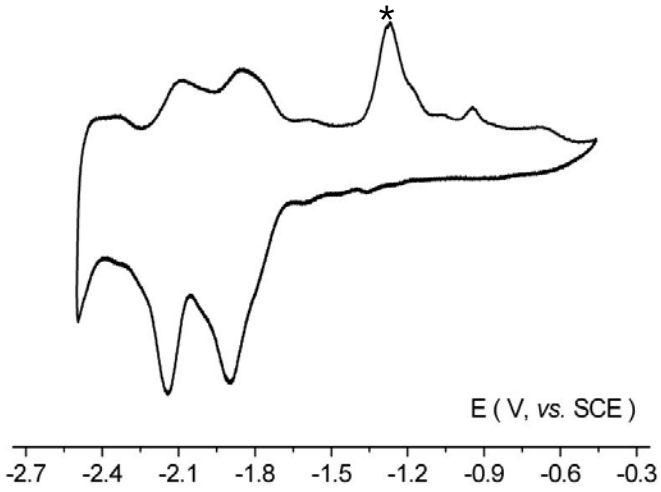

Figure S2. First derivative deconvolute voltammetric response recorded at a gold electrode in THF solution of $\mathbf{4}^{2-}$ ($0.8 \cdot 10^{-3}$ mol dm^{-3}). Experimental conditions illustrated in Figure 6.

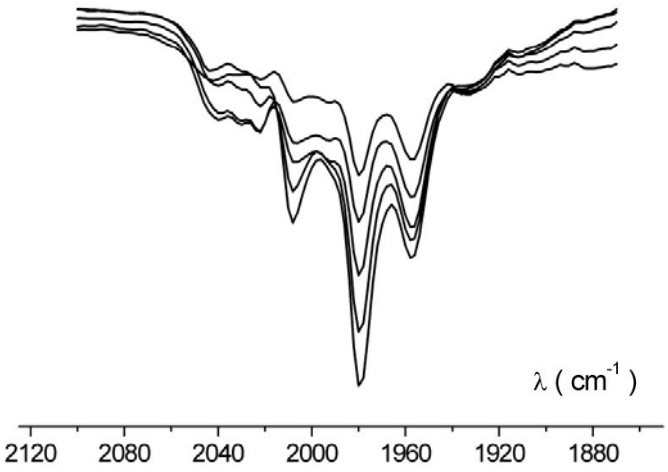

Figure S3. Infrared spectro-electrochemical trends (in correspondence of the region of the terminal ν_{CO} frequencies) recorded in OTTLE cell in THF solution of **4** after the first oxidation.

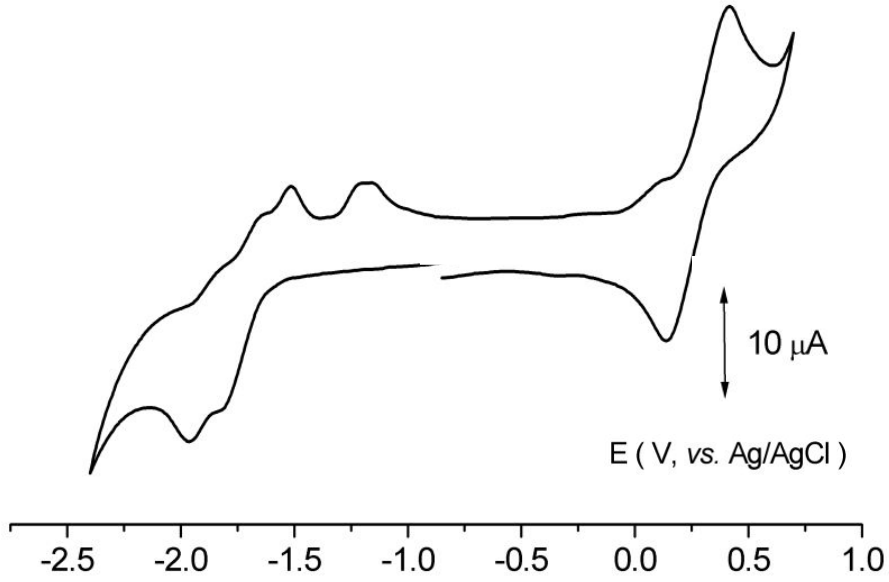

Figure S4. Cyclic voltammogram recorded at a platinum electrode in THF solution of $[Fe_4C(CO)_{12}(CuNC_5H_5)]^-$ (1.4×10^{-3} M). $[NBu_4][PF_6]$ (0.2 M) supporting electrolyte. Scan rate 0.20 Vs^{-1}. Temperature 273 K.

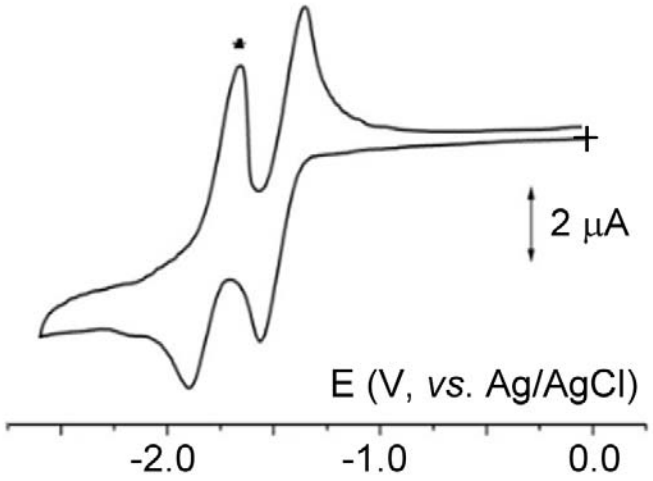

Figure S5. Cyclic voltammetric response recorded at a glassy carbon electrode in THF solution of 7^{2-} ($0.5 \cdot 10^{-3}$ mol dm^{-3}). $[NBu_4][PF_6]$ ($0.2 \cdot 10^{-3}$ mol dm^{-3}) supporting electrolyte. Scan rate 0.02 V s^{-1}. Temperature 253 K.

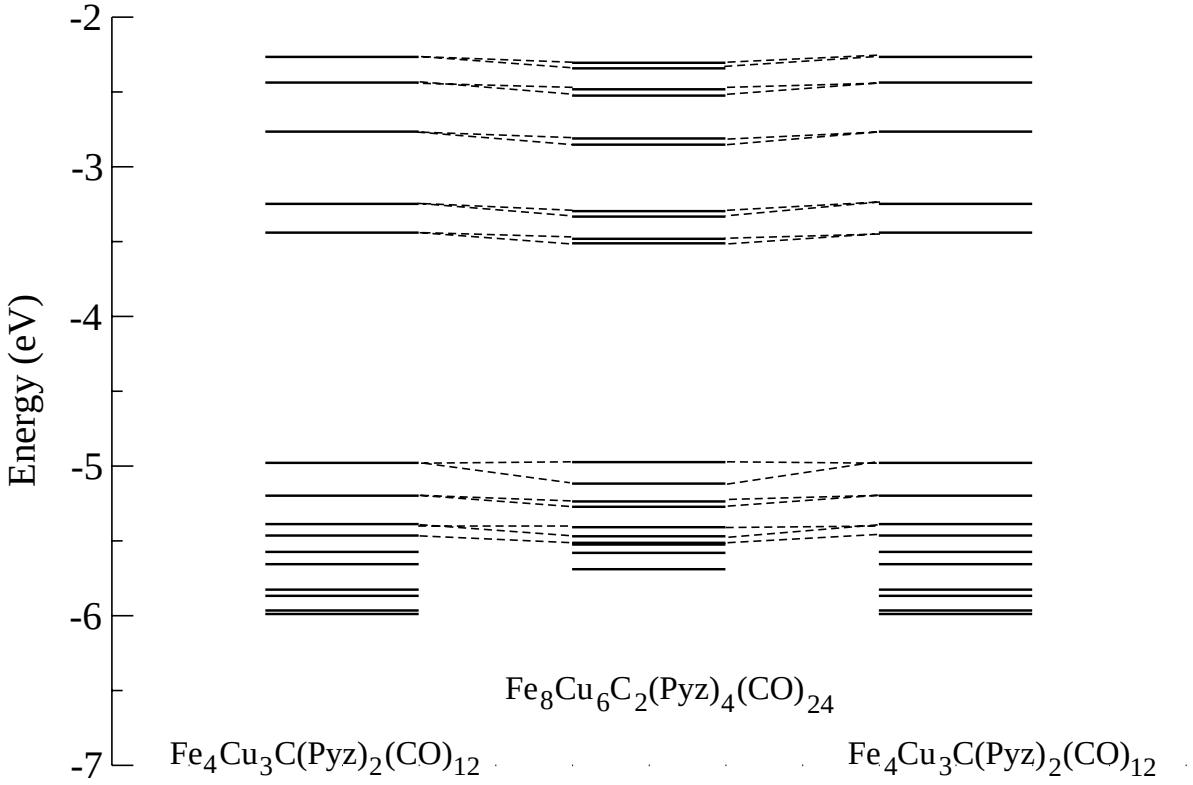

Figure S6 Orbital correlation diagram for cluster **$[NEt_4]_2$7**.

Table S1 – X-ray selected interatomic distances (Å) and angles (°) for $[\{Fe_4C(CO)_{14}Cu\}_2(\mu\text{-ddpe})]^{2-}$ (**3**) and $[\{Fe_4C(CO)_{14}Cu\}_2(\mu\text{-pyz})]^{2-}$ (**4**) $[Fe_4C(CO)_{14}Cupy]^-$ (**5**) with Estimated Standard Deviations (e.s.d.'s) in parentheses.

	3 X = P	4 X = N	5 X = N
Cu1-Fe1	3.156(1)	2.648(1)	3.178(1)
Cu1-Fe3	2.593(1)	2.577(1)	2.589(1)
Cu1-Fe4	2.603(1)	2.614(1)	2.581(1)
Fe1-Fe2	2.531(1)	2.528(1)	2.527(1)
Fe1-Fe3	2.649(1)	2.690(1)	2.646(1)
Fe1-Fe4	2.653(1)	2.690(1)	2.669(1)
Fe2-Fe3	2.673(1)	2.673(1)	2.681(1)
Fe2-Fe4	2.692(1)	2.677(1)	2.669(1)
Cu-C	1.901(2)	1.887(3)	1.863(2)
Fe1-C	1.978(3)	1.984(2)	1.953(2)
Fe2-C	1.891(2)	1.926(3)	1.906(3)
Fe3-C	1.835(3)	1.823(3)	1.830(2)
Fe4-C	1.825(3)	1.817(3)	1.830(2)
Cu-X1	2.210(1)	1.939(3)	1.926(2)
C-Cu-X1	172.7(1)	174.4(1)	179.3(1)

Table S2 – X-ray selected interatomic distances (Å) and angles (°) for $[Fe_4Cu_3C(CO)_{12}(\mu\text{-}S_2CNEt_2)_2]^-$ (**6**) and $[\{Fe_4Cu_3C(CO)_{12}(\mu\text{-}pz)_2\}_2]^{2-}$ (**7**) with Estimated Standard Deviations (e.s.d.'s) in parentheses.

	6 X = S	7 X = N
Cu1-Cu2	2.629(1)	2.663(1)
Cu1-Cu3	2.779(1)	3.105(1)
Cu2-Cu3	2.892(1)	3.124(1)
Cu3-Cu6		2.749(1)
Cu4-Cu5		2.691(1)
Cu4-Cu6		3.084(1)
Cu5-Cu6		3.127(1)
Cu1-Fe1	2.958(1)	2.899(1)
Cu1-Fe3	2.623(1)	2.608(1)
Cu1-Fe4	2.691(1)	2.663(1)
Cu2-Fe2	2.713(1)	2.647(1)
Cu2-Fe3	2.719(1)	2.670(1)
Cu2-Fe4	2.661(1)	2.636(1)
Cu4-Fe5		2.907(1)
Cu4-Fe7		2.620(1)
Cu4-Fe8		2.629(1)
Cu5-Fe6		2.619(1)
Cu5-Fe7		2.643(1)
Cu5-Fe8		2.698(1)
Fe1-Fe2	2.555(1)	2.562(1)
Fe1-Fe3	2.697(1)	2.692(1)
Fe1-Fe4	2.639(1)	2.684(1)
Fe2-Fe3	2.699(1)	2.681(1)
Fe2-Fe4	2.689(1)	2.717(1)
Fe5-Fe6		2.553(1)
Fe5-Fe7		2.701(1)
Fe5-Fe8		2.669(1)
Fe6-Fe7		2.705(1)
Fe6-Fe8		2.705(1)
Cu1-C	1.908(2)	1.882(3)
Cu2-C	1.910(2)	1.893(3)
Cu4-C'		1.884(3)
Cu5-C'		1.903(3)
Fe1-C	1.939(2)	1.924(3)
Fe2-C	1.931(2)	1.930(3)
Fe3-C	1.865(2)	1.874(3)
Fe4-C	1.861(2)	1.858(3)
Fe5-C'		1.926(3)
Fe6-C'		1.915(3)
Fe7-C'		1.871(3)
Fe8-C'		1.867(3)
Cu1-X1	2.185(1)	1.887(3)
Cu2-X2	2.173(1)	1.892(3)
Cu3-X3	2.196(1)	1.861(3)
Cu3-X4	2.173(1)	1.856(3)
Cu4-N6		1.886(3)
Cu5-N5		1.893(3)
Cu6-N7		1.864(3)
Cu6-N8		1.864(3)
C-Cu1-X1	177.91(6)	171.7(1)
C-Cu2-X2	175.02(6)	170.1(1)
X3-Cu3-X4	157.34(3)	175.6(1)
C'-Cu4-N6		171.7(1)
C'-Cu5-N5		169.9(1)
N7-Cu6-N8		176.4(1)

Table S3 - Selected interatomic distances (Å) and angles (°) obtained with BP86/def-TZVP for the optimized structures of $[\{Fe_4C(CO)_{14}Cu\}_2(\mu\text{-ddpe})]^{2-}$ (**3**) and $[\{Fe_4C(CO)_{14}Cu\}_2(\mu\text{-pyz})]^{2-}$ (**4**) $[Fe_4C(CO)_{14}Cupy]^-$ (**5**), $[Fe_4C(CO)_{14}Cupyz]^-$ (**5a**), and $[Fe_4C(CO)_{14}CuCl]^{2-}$ (**5b**). Here, sp and bp indicates the square pyramid and *arachno*-pentagonal bipyramids conformations, respectively.

	3 X = P		4 X = N		5 X = N		5a X = N		5b X = Cl	
	sp	**bp**	**sp**	**bp**	**sp**	**bp**	**sp**	**bp**	**sp**	**bp**
Cu1-Fe1	2.760	3.126	2.647	3.600	2.629	3.583	2.625	3.548	2.768	3.549
Cu1-Fe3	2.619	2.601	2.577	2.579	2.613	2.575	2.610	2.573	2.693	2.704
Cu1-Fe4	2.631	2.623	2.617	2.587	2.571	2.578	2.566	2.568	2.582	2.579
Fe1-Fe2	2.557	2.553	2.563	2.548	2.562	2.554	2.563	2.552	2.557	2.549
Fe1-Fe3	2.664	2.671	2.697	2.720	2.683	2.702	2.683	2.707	2.679	2.683
Fe1-Fe4	2.667	2.675	2.683	2.723	2.707	2.725	2.707	2.729	2.710	2.704
Fe2-Fe3	2.703	2.718	2.697	2.703	2.716	2.725	2.718	2.724	2.697	2.703
Fe2-Fe4	2.695	2.706	2.710	2.723	2.700	2.702	2.704	2.702	2.683	2.682
Cu-C	1.941	1.922	1.917	1.896	1.918	1.886	1.919	1.891	1.917	1.895
Fe1-C	1.996	1.979	1.997	1.923	1.998	1.917	1.996	1.916	1.988	1.953
Fe2-C	1.913	1.909	1.904	1.925	1.903	1.924	1.901	1.918	1.930	1.945
Fe3-C	1.843	1.845	1.844	1.845	1.840	1.849	1.839	1.847	1.845	1.848
Fe4-C	1.845	1.845	1.840	1.845	1.843	1.849	1.843	1.847	1.846	1.854
Cu-X1	2.280	2.267	1.943	1.927	1.954	1.933	1.941	1.921	2.206	2.198

Table S4 - Selected interatomic distances (Å) and angles (°) obtained with BP86/def-TZVP for the optimized structures of $[\{Fe_4Cu_3C(CO)_{12}(\mu\text{-}pz)_2\}_2]^{2-}$ (**[NEt$_4$]$_2$7**).

Cu1-Cu2	2.757
Cu1-Cu3	3.164
Cu2-Cu3	3.191
Cu3-Cu6	2.870
Cu4-Cu5	2.760
Cu4-Cu6	3.174
Cu5-Cu6	.183
Cu1-Fe1	2.835
Cu1-Fe3	2.607
Cu1-Fe4	2.663
Cu2-Fe2	2.666
Cu2-Fe3	2.701
Cu2-Fe4	2.636
Cu4-Fe5	2.831
Cu4-Fe7	2.588
Cu4-Fe8	2.682
Cu5-Fe6	2.658
Cu5-Fe7	2.626
Cu5-Fe8	2.709
Fe1-Fe2	2.593
Fe1-Fe3	2.718
Fe1-Fe4	2.711
Fe2-Fe3	2.723
Fe2-Fe4	2.744
Fe5-Fe6	2.596
Fe5-Fe7	2.733
Fe5-Fe8	2.698
Fe6-Fe7	2.739
Fe6-Fe8	2.726
Cu1-C	1.904
Cu2-C	1.916
Cu4-C’	1.904
Cu5-C’	1.915
Fe1-C	1.929
Fe2-C	1.928
Fe3-C	1.881
Fe4-C	1.879
Fe5-C’	1.915
Fe6-C’	1.904
Fe7-C’	1.879
Fe8-C’	1.884
Cu1-N1	1.922
Cu2-N2	1.922
Cu3-N3	1.884
Cu3-N4	1.888
Cu4-N6	1.918
Cu5-N5	1.921
Cu6-N7	1.886
Cu6-N8	1.887
C-Cu1-N1	167.7
C-Cu2-N2	166.7
N3-Cu3-N4	174.1
C’-Cu4-N6	166.5
C’-Cu5-N5	166.3
N7-Cu6-N8	173.9

Table S5 - Mean unsigned deviation (MUD) for all Cu-Fe, Fe-Fe, Fe(Cu)-C, Cu-Cu and Cu-X1 distances (Å) the optimized structures of $[\{Fe_4C(CO)_{14}Cu\}_2(\mu\text{-ddpe})]^{2-}$ (**3**) and $[\{Fe_4C(CO)_{14}Cu\}_2(\mu\text{-pyz})]^{2-}$ (**4**) $[Fe_4C(CO)_{14}Cupy]^-$ (**5**), $[Fe_4C(CO)_{14}Cupyz]^-$ (**5a**), $[Fe_4C(CO)_{14}CuCl]^{2-}$ (**5b**), and $[\{Fe_4Cu_3C(CO)_{12}(\mu\text{-pz})_2\}_2]^{2-}$ (**$[NEt_4]_2$7**). Here, sp and bp indicates the square pyramid and *arachno*-pentagonal bipyramids conformations, respectively. For the Cu-Fe distances in parenthesis is reported the MUD calculated by excluding the Cu-Fe1 distance

		Cu-Fe	Fe-Fe	Fe(Cu)-C	Cu-X1	Cu-Cu
3	**sp**	0.150 (0.027)	0.018	0.022	0.070	
	bp	0.016 (0.014)	0.025	0.014	0.057	
4	**sp**	0.001 (0.001)	0.021	0.022	0.004	
	bp	0.327 (0.015)	0.053	0.024	0.012	
5	**sp**	0.194 (0.017)	0.035	0.025	0.028	
	bp	0.141 (0.009)	0.043	0.023	0.007	
$[NEt_4]_2$7		0.036	0.031	0.013	0.028	0.079

Table S6 - Energies (in Hartree) of the optimized structures of **3**, **4**, **5**, **5a**, **5b**, **$[NEt_4]$7-mon**, and **$[NEt_4]_2$7** computed at BP86/def-TZVP level of theory. All calculations have been performed in *vacuum*, with the exception of **$[NEt_4]$7-mon** and **$[NEt_4]_2$7** which have been modeled according to the COSMO approach, by considering a *polarizable continuum medium* characterized by the ε value of solvent THF.

	sp	**bp**
3	-17880.25628028530	-17880.25587145851
4	-16456.31451921766	-16456.30822802507
5	-8344.34151812727	-8344.33566812146
5a	-8360.38512151495	-8360.38093192997
5b	-8556.26505139971	-8556.26494256457
$[NEt_4]$7-mon	-12200.80634189945	
$[NEt_4]_2$7	-24401.61403350897	